Hyperfine structure of Sc II: Experiment and theory

L. Young, W. J. Childs, T. Dinneen, C. Kurtz, H. G. Berry, and L. Engström*
Physics Division, Argonne National Laboratory, Argonne, Illinois 60439

K. T. Cheng
Lawrence Livermore National Laboratory, Livermore, California 94550
(Received 26 October 1987)

Collinear laser–ion-beam spectroscopy has been used to measure hyperfine structure (hfs) in three levels of the $3d^2$ and six levels of the $3d4p$ configuration of Sc II. The results combine with earlier measurements of hfs within these configurations to give a fairly complete picture of hfs in these configurations. The combined results are compared with multiconfiguration Dirac-Fock (MCDF) *ab initio* calculations. Good agreement is obtained for the magnetic dipole hfs constants of the singlet states in both the $3d^2$ and $3d4p$ configurations, but the MCDF predictions for the triplet states are not even qualitatively correct. The poor agreement for the triplet states appears to be due to the neglect of core polarization in the present MCDF approach.

INTRODUCTION

During the past decade there has been an exploitation of collinear laser–ion-beam spectroscopy to study hyperfine structure (hfs) of atoms in low-ionization stages.[1–3] Most of the activity has focused on the acquisition of nuclear data (dipole and quadrupole moments). Despite the fact that the nuclear parameters inferred from hfs depend critically on evaluation of the electronic wave functions and $\langle r^{-3} \rangle$ values, relatively little emphasis has been placed on understanding, at an *ab initio* level, the atomic aspects of the problem. To date, detailed experimental and theoretical analyses of hfs of singly ionized atoms have dealt primarily with complicated systems, such as Er II.[4] Here we have studied both experimentally and theoretically the hfs of a somewhat simpler and much lighter system with only two valence electrons, Sc II.

Sc II turns out to be an interesting atom for testing *ab initio* calculations. In Sc II, the $3d$ and $4s$ orbits compete for the lowest energy,[5] resulting in a host of even-parity metastable states arising from the $3d^2$ and $3d4s$ configurations which are easily accessible by experiment. The situation is quite different in the isoelectronic neutral Ca, where the $4s4p$ configuration lies between the ground $4s^2$ and $4s3d$ configurations. The result, for Sc II, is that a large number of levels from the $3d^2$ and $3d4p$ configurations are accessible using standard single-photon techniques. In fact, numerous oscillator-strength measurements,[6–10] which are sensitive to a different portion of the electronic wave function, have been performed on the $3d4p$ odd-parity levels. The wealth of data available for these low-lying levels of this quasi-two-electron system makes Sc II an attractive place to study single-particle and pair correlation effects, as has been done for Ca I.[11,12]

In this paper, we report on the measurement of hfs in five new levels of Sc II arising from the $3d^2$ and $3d4p$ configurations using the collinear laser–ion-beam method. The present results, combined with the one earlier measurement of hfs in Sc II by Arnesen *et al.*,[13] produce a fairly complete picture of hfs in the $3d^2$ and $3d4p$ configurations in Sc II. We also report *ab initio* multiconfiguration Dirac-Fock (MCDF) calculations, not including core polarization, for all experimentally measured states. A comparison of experimental and MCDF results suggests that core polarization plays an important role in the hfs of these configurations.

EXPERIMENTAL

The scandium ions were produced in an oscillating electron-impact ionization source by flowing CCl_4 over Sc_2O_3. Ions were extracted through a 0.8-mm hole, accelerated to 50 keV and mass separated with a 90° analyzing magnet. Additional focusing of the mass-selected $^{45}Sc^+$ beam produced a collimated beam suitable for collinear interaction with a laser beam. Typical beam currents during the experiments were 1.0 μA, corresponding to a number density in the interaction region of $\approx 1.7 \times 10^5$ ions/cm^3. The transit time to the interaction region was ≈ 10 μs. Therefore, the metastable even-parity levels arising from the $3d^2$, $3d4s$, and $4s^2$ configurations which were populated in the source survived to the interaction region.

The output of an actively stabilized ring dye laser (rms bandwidth less than 1 MHz) was superimposed collinearly with the ion beam. Laser-induced fluorescence (LIF) from a 2.5 cm length of the ion beam was imaged onto a photomultiplier tube. Details of the interaction region have been previously described.[14] LIF spectra were obtained by scanning the laser with the observation region held at an arbitrary nonzero voltage, and normalizing to beam current. Frequency markers (150 MHz) were obtained by passing some of the laser light through a temperature-stabilized confocal Fabry-Perot etalon. The etalon had been previously calibrated.[14] The absolute wavelength of the laser was determined with a scanning

TABLE I. Lines studied in Sc II.

Laser λ in air (Å)	Even-parity lower level Configuration	Excitation energy (cm^{-1})	*SLJ*	Odd-parity upper level Configuration	Excitation energy (cm^{-1})	*SLJ*	Filter (Å)
6059.24	$3d^2$	10944.56	$^1D_2$	$3d4p$	27443.41	$^3F^\circ_2$	3600
6001.50	$3d^2$	10944.56	$^1D_2$	$3d4p$	27602.45	$^3F^\circ_3$	3600
5890.01	$3d^2$	10944.56	$^1D_2$	$3d4p$	27917.78	$^3D^\circ_1$	3600
5657.90	$3d^2$	12154.42	$^3P_2$	$3d4p$	29823.93	$^3P^\circ_2$	3400
5684.21	$3d^2$	12154.42	$^3P_2$	$3d4p$	29742.16	$^3P^\circ_1$	3600
5526.80	$3d^2$	14261.32	$^1G_4$	$3d4p$	32349.98	$^1F^\circ_3$	3600

Michelson wavemeter.

The atomic lines studied are listed in Table I. The first column lists the wavelength (in air) of the transition. Columns 2–7 describe the lower and upper levels connected by the laser. Column 8 lists the interference filter used to isolate the decay channel. All lower levels studied arise from the $3d^2$ configuration, and all upper levels from the $3d4p$ configuration. All but the 6001-Å line are listed in the most recent compilation[5] of the spectrum of Sc II. Five of the nine levels shown in Table I had not previously been studied in enough detail to reveal hfs.

In Fig. 1 all of the levels of the $3d^2$ and $3d4p$ configurations which have been studied by collinear laser–ion-beam spectroscopy are shown. Fluorescence decay from the laser-excited $3d4p$ levels to the ground $3d4s$ configuration was monitored in all cases. Combining the earlier work of Arnesen *et al.*[13] with the present results, hfs in 4 of 7 possible levels in the $3d^2$ configuration and in 9 of 11 possible levels in the $3d4p$ configuration has now been measured. Two of the lines studied, $^1D_2-^3F^\circ_2$ and $^1D_2-^3F^\circ_3$, were quite weak and required substantial laser power ($\approx$200 mW) to be measured. The other lines were easily observable with less than 10 mW.

A typical LIF scan is shown in Fig. 2. In this particular transition, $^3P_2$ (12154 cm^{-1})–$^3P^\circ_2$ (29823 cm^{-1}), all hfs components are clearly resolved. The linewidth [full width at half maximum (FWHM)] of $\approx$50 MHz results

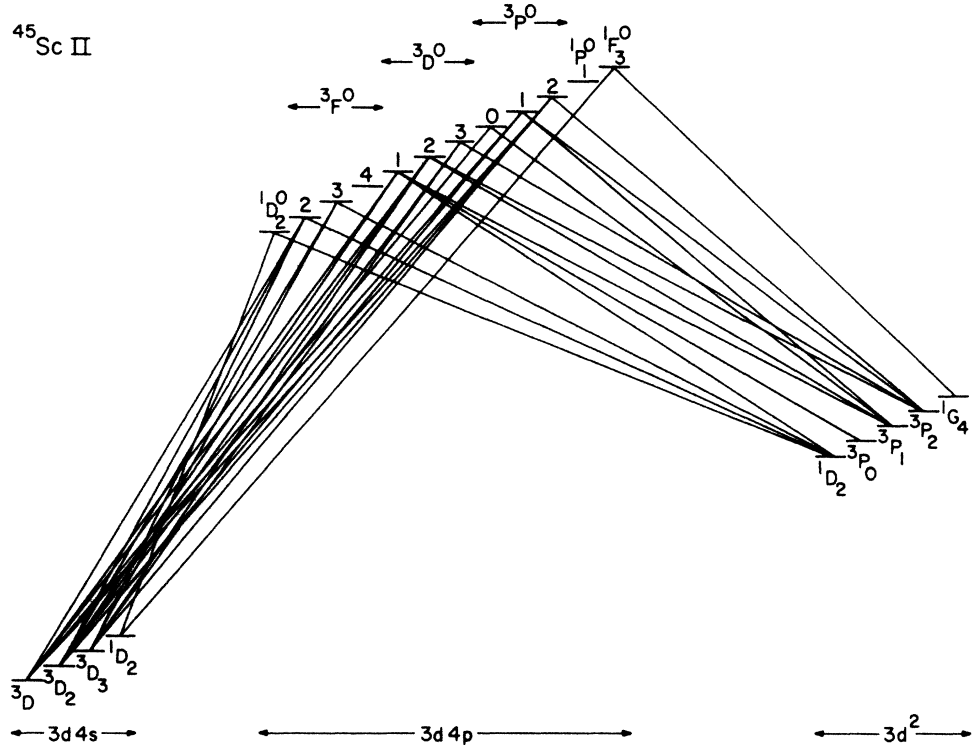

FIG. 1. Partial-energy-level diagram showing the levels within the $3d^2$ and $3d4p$ configurations which have been studied using collinear laser–ion-beam spectroscopy. Fluorescence decay from the laser excited $3d4p$ levels to the ground $3d4s$ configuration was monitored in all cases.

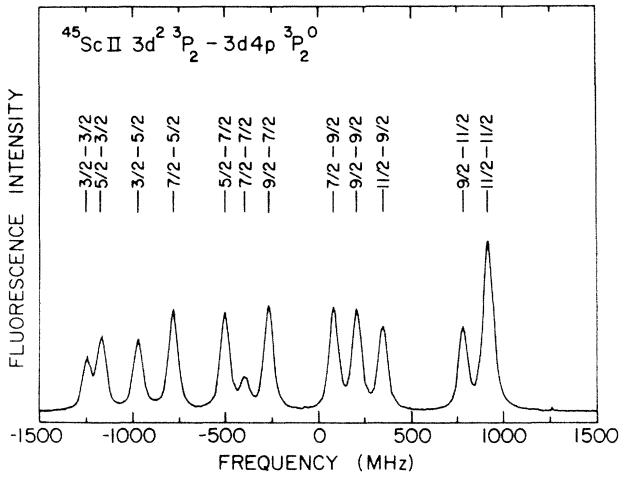

FIG. 2. Laser-induced fluorescence spectrum of the $3d^2\,{}^3P_2-3d4p\,{}^3P_2^\circ$ transition in Sc II.

from (1) transit time broadening ($\approx$20 MHz), (2) lifetime broadening ($\approx$16 MHz), and (3) ion-source energy spread. The observed linewidth is between three to four times smaller than that previously reported by Arnesen *et al.* This is presumably due to the extremely high stability of our accelerating voltage ($dE/E \approx 2\times 10^{-6}$).

RESULTS

The experimentally measured hyperfine splittings have been analyzed using the standard expressions for the hfs interaction energy:

$$E_{\rm hfs} = A\frac{K}{2} + B\frac{3K(K+1)-4I(I+1)J(J+1)}{8I(2I-1)J(2J-1)},$$

where $K=F(F+1)-I(I+1)-J(J+1)$, A is the magnetic dipole, and B the electric quadrupole coupling constant.

Table II lists the A and B hfs constants determined for ^{45}Sc II by collinear laser–ion-beam spectroscopy. The present results, as well as those of Arnesen *et al.*, are collected in this table. The A and B values presented are weighted averages of several measurements. The uncertainties quoted represent one standard deviation of the mean. The rather large uncertainties arise from random fluctuations in the acceleration voltage, which are in turn probably due to fluctuations in the ion-source operating conditions. These fluctuations are easily seen through the internal consistency of each run. A change of 1 V in the acceleration voltage will shift the resonance position by $\approx$7.9 MHz, a non-negligible amount since peak positions can be determined within $\pm$2 MHz. These shifts in acceleration voltage could not be accounted for in the present data analysis. A typical rms deviation for 12 observations fitted with four parameters in a single run was 3 MHz. Although it was not our purpose in this study to remeasure hfs in those levels previously studied,[13] we report a few repeated measurements here as well as new results for five levels. In some cases, e.g., $3d^2\,{}^1D_2$ (10 944 cm^{-1}), there is a small disagreement between present and earlier results. This disagreement is most likely due to considerable line blending in the earlier measurement.

INTERPRETATION AND COMPARISON WITH THEORY

Before proceeding with a detailed comparison of experiment with theory, it is informative to summarize the level structure of the low-lying even and odd configurations in Sc II. The ground configuration in Sc II is $3d4s$, which

TABLE II. Hfs constants determined for ^{45}Sc II by fast-ion-beam laser spectroscopy.

Level (cm^{-1})	Configuration	SLJ	hfs constants[a] (MHz) A	B
10 944.56	$3d^2$	$^1D_2$	149.9(3)	2(6)
			151.8(6)[b]	12(6)[b]
12 101.50	$3d^2$	$^3P_1$	−107.3(6)[b]	−9(3)[b]
12 154.42	$3d^2$	$^3P_2$	−27.9(4)	19(6)
			−27.7(8)[b]	8(8)[b]
14 261.32	$3d^2$	$^1G_4$	135.2(1.6)	−52(32)
26 081.34	$3d4p$	$^1D_2^\circ$	215.7(8)[b]	18(7)[b]
27 443.71	$3d4p$	$^3F_2^\circ$	366.8(1.1)	−40(14)
27 602.45	$3d4p$	$^3F_3^\circ$	205.4(6)	−70(18)
27 917.78	$3d4p$	$^3D_1^\circ$	303.2(1.5)	10(5)
			304.3(8)[b]	2(3)[b]
28 021.29	$3d4p$	$^3D_2^\circ$	125.4(1.0)[b]	7(7)[b]
28 161.17	$3d4p$	$^3D_3^\circ$	101.4(6)[b]	−23(12)[b]
29 742.16	$3d4p$	$^3P_1^\circ$	255.0(2.4)	10(8)
			257.7(1.4)[b]	9(6)[b]
29 823.93	$3d4p$	$^3P_2^\circ$	106.3(9)	−24(18)
32 349.98	$3d4p$	$^1F_3^\circ$	190.6(2.1)	−69(34)

[a]Present work except where noted.
[b]Reference 13.

TABLE III. Effective operator expressions for the A values of the $3d^2$ and $3d4p$ configurations in Sc II. The experimental A values shown on the right are weighted averages of the values presented in Table II.

$A(3d^2\,{}^1D_2)$	$=1.000a_{3d}$			$=150.3$ MHz
$A(3d^2\,{}^3P_1)$	$=$		$0.500C'$	$=-107.3$ MHz
$A(3d^2\,{}^3P_2)$	$=0.600a_{3d}$		$+0.500C'$	$=-27.9$ MHz
$A(3d^2\,{}^1G_4)$	$=1.000a_{3d}$			$=135.2$ MHz
$A(3d4p\,{}^1D_2)$	$=0.833a_{3d}$	$+0.167a_{4p}$		$=215.7$ MHz
$A(3d4p\,{}^3F_2)$	$=1.118a_{3d}$	$+0.604a_{4p}$	$-0.167C$	$=366.8$ MHz
$A(3d4p\,{}^3F_3)$	$=0.683a_{3d}$	$+0.356a_{4p}$	$+0.042C$	$=205.4$ MHz
$A(3d4p\,{}^3D_1)$	$=1.500a_{3d}$	$-0.100a_{4p}$	$-0.250C$	$=304.0$ MHz
$A(3d4p\,{}^3D_2)$	$=0.778a_{3d}$	$+0.022a_{4p}$	$+0.083C$	$=125.4$ MHz
$A(3d4p\,{}^3D_3)$	$=0.508a_{3d}$	$+0.178a_{4p}$	$+0.167C$	$=101.4$ MHz
$A(3d4p\,{}^3P_1)$	$=1.000a_{3d}$	$-0.200a_{4p}$	$+0.250C$	$=257.0$ MHz
$A(3d4p\,{}^3P_2)$	$=0.700a_{3d}$	$-0.260a_{4p}$	$+0.250C$	$=106.3$ MHz
$A(3d4p\,{}^1F_3)$	$=0.667a_{3d}$	$+0.333a_{4p}$		$=190.6$ MHz

where $C'=a^{10}_{3d}$ and $C=a^{10}_{3d}+a^{10}_{4p}$

accounts for the four lowest levels ranging from 0 to 2541 cm^{-1}. The next higher configuration is $3d^2$, the levels of which range from 4803 to 25 955 cm^{-1}. The level $4s^2$ ($^1S_0$) lies in the middle of the $3d^2$ configuration at 11 736 cm^{-1}. The next even-parity level arises from the $3d5s$ configuration and lies at 57 552 cm^{-1}. As for the low-lying odd-parity levels, the first 12 arise from the $3d4p$ configuration and range from 26 081 to 32 350 cm^{-1}. All the levels of $3d4p$ have clear LS character, being more than 90% pure in all cases.[5] We will now discuss hfs in the $3d^2$ and $3d4p$ configurations in terms of the effective operator method of Sandars and Beck and *ab initio* MCDF calculations.

Semiempirical effective operator approach

Although the emphasis in this paper is not on an interpretation of hfs by the semiempirical effective-operator (EO) method, it is instructive to examine the data in this framework. In the Sandars-Beck effective operator theory,[15] the lowest-order hfs interaction, the magnetic dipole interaction, for a single valence electron is represented by

$$H_{\rm hfs}({\rm M1})=[a^{01}_{nl}\mathbf{l}-\sqrt{10}a^{12}_{nl}(\mathbf{s}\times\mathbf{C}^{(2)})^{(1)}+a^{10}_{nl}\mathbf{s}]\cdot\mathbf{I}\ ,$$

where $\mathbf{C}^{(2)}$ is the spherical tensor of order 2 and

$$a_{nl}=2\mu_B\mu_N(\mu_I/I)\langle r^{-3}\rangle\ .$$

In the EO approach, the expectation values of the radial parts of the operators are treated as adjustable parameters used to fit the observed hfs. Since $H_{\rm hfs}$(M1) is a single particle operator, each open shell requires a separate set of three parameters (a^{01},a^{12},a^{10}) to describe the magnetic dipole interaction. Thus for the $3d^2$ configuration three parameters are required and for the $3d4p$ configuration six parameters are required.

In order to evaluate the magnetic dipole hfs constants for the $3d^2$ and $3d4p$ configurations, we make the following simplifications. First we assume that $a^{01}=a^{12}$, as is rigorously true in the nonrelativistic limit and in the absence of configuration interaction. Second, we treat all states as 100% pure LS coupled.

With these simplifications, the EO expressions for the A values of the $3d^2$ and $3d4p$ configurations can be evaluated[16] and are shown in Table III. In the expressions shown in Table III, the experimental A values on the right are weighted averages of the values presented in Table II.

For the $3d^2$ configuration, two parameters a_{3d} and C' are used to fit four observations. A least-squares fit yields the values $a_{3d}=141.9$ MHz and $C'=-220.3$ MHz, with a rms deviation of 5 MHz.

For the $3d4p$ configuration, three parameters (a_{3d}, a_{4p}, and C) are used to fit the nine observations. A least-squares fit yields the values $a_{3d}=223.5$ MHz, $a_{4p}=148.0$ MHz, and $C=6.6$ MHz. The large rms deviation (32 MHz) for this set of observations is probably due to deviation from pure LS coupling for the states in question.

Nevertheless, from these two fits we can gain considerable insight. From the $3d^2$ levels, we obtain a value of $C'=-220.3$ MHz for the contact contribution of a $3d$ electron. Since there are no s or $p_{1/2}$ electrons in this configuration, one would initially expect this contact con-

TABLE IV. Effective operator expressions for the B values of the $3d^2$ and $3d4p$ configurations of Sc II.

$B(3d^2\,{}^1D_2)$	$=-0.245b_{3d}$		$=7$ MHz
$B(3d^2\,{}^3P_1)$	$=0.200b_{3d}$		$=-9$ MHz
$B(3d^2\,{}^3P_2)$	$=-0.400b_{3d}$		$=14$ MHz
$B(3d^2\,{}^1G_4)$	$=1.143b_{3d}$		$=-52$ MHz
$B(3d4p\,{}^1D_2)$	$=0.286b_{3d}$	$-0.400b_{4p}$	$=18$ MHz
$B(3d4p\,{}^3F_2)$	$=0.392b_{3d}$	$+0.274b_{4p}$	$=-40$ MHz
$B(3d4p\,{}^3F_2)$	$=0.429b_{3d}$	$+0.300b_{4p}$	$=-70$ MHz
$B(3d4p\,{}^3D_1)$	$=0.100b_{3d}$	$-0.140b_{4p}$	$=4$ MHz
$B(3d4p\,{}^3D_2)$	$=0.143b_{3d}$	$-0.200b_{4p}$	$=7$ MHz
$B(3d4p\,{}^3D_3)$	$=0.286b_{3d}$	$-0.400b_{4p}$	$=-23$ MHz
$B(3d4p\,{}^3P_1)$	$=-0.100b_{3d}$	$-0.020b_{4p}$	$=9$ MHz
$B(3d4p\,{}^3P_2)$	$=0.200b_{3d}$	$+0.040b_{4p}$	$=-24$ MHz
$B(3d4p\,{}^3F_3)$	$=0.429b_{3d}$	$+0.300b_{4p}$	$=-69$ MHz

tribution to be small. From the quantity $C-C'$, one deduces that the contact contribution of the $4p$ electron is $+226.9$ MHz. Thus the contact contribution of the $4p$ electron is *large and opposite in sign* to that of the $3d$ electron.

Similarly, in the nonrelativistic limit, EO expressions for the B values can be derived. All 13 observations are fitted with two parameters, b_{3d} and b_{4p}. The expressions for the B values are shown in Table IV. A least-squares fit to the entire set of observations yields the values $b_{3d}=-60.8$ MHz and $b_{4p}=-74.6$ MHz and a rms deviation of 10 MHz. Relative to the experimental uncertainties (± 15 MHz), the B values are fit essentially to within experimental error.

Multiconfiguration Dirac-Fock *ab initio* treatment

The MCDF treatment of hfs has been described in detail previously.[17] Briefly, the MCDF eigenenergies and wave functions were obtained using a relativistic self-consistent-field calculation[18] within a given set of configurations and basis orbitals. After proper identification of the state in terms of its energy, parity, and J value, matrix elements of the hyperfine Hamiltonian are evaluated. From the known values of the nuclear moments,[19] μ_I and Q, the A and B values are calculated and can be compared with experiment.

Table V lists the experimental and MCDF values for the magnetic dipole hfs constant. For the even-parity states, the tabulated MCDF values were obtained by using only the $3d^2$ configurations in the calculation. Similarly, for the odd-parity states, the values were obtained by using only the $3d4p$ configurations. In the last column, the difference between calculated MCDF and observed values is shown in percent. It is obvious from this column that agreement between experiment and theory is spotty at best.

A closer examination of Table V, however, reveals that the agreement for the singlet levels is much better than for the triplet levels. The deviation, in all four cases in both $3d^2$ and $3d4p$ configurations, is less than 7%. However, the A values calculated for the triplet levels show considerable disagreement from experiment, particularly within the $3d^2$ configuration.

This can be understood by recalling that the "contact" contribution to the A values arises from an $\mathbf{s}\cdot\mathbf{I}$ interaction, and is therefore proportional to g_J-1.[20] Since (g_J-1) equals zero for singlet states where $J=L$, any neglect of factors contributing to a nonzero contact term would not appear in the calculated A values of these states. In other words, a nonzero contact contribution would affect the calculated A values of the triplets, but not the singlets. This can also be seen from the EO expressions for the A values (Table III).

In the $3d^2$ configuration, we note also that the values of $A_{\text{obs}}-A_{\text{calc}}$ are substantial and nearly equal (≈ 110 MHz) for the $^3P_{1,2}$ states. This behavior is also consistent with a (g_J-1)-type contact contribution to the A values, since the g_J values for $^3P_1$ and $^3P_2$ are identical (see Table III). Contact hfs is also important in the triplet states of the $3d4p$ configuration, but the effects are less clear-cut.

The question naturally arises as to the origin of the contact contribution in these configurations involving only d and p electrons. The two obvious candidates are configuration interaction (CI) between the two valence electrons and core polarization (CP). We first consider configuration interaction. Although not shown in Table V, MCDF calculations were also made with an expanded set of configurations for the even-parity $3d^2$ levels. The expanded set included all combinations of $(3d+4s+4p)^2$ configurations. The results for the A values of the triplet states were virtually identical (within 5%) to those obtained using only $3d^2$. The discrepancies are as large as 400%. Even though this is by no means an exhaustive study of possible configuration interaction effects between the two valence electrons, the fact that allowing an unpaired $4s$ electron in the calculation has almost no effect on the dipole hfs strongly suggests that CI is not the

TABLE V. Comparison of observed A values with *ab initio* MCDF values.

Level (cm^{-1})	Configuration	SLJ	A values (MHz) A (observed)[a]	A (MCDF)[b]	Δ (%)
10 944.56	$3d^2$	$^1D_2$	150.3	146.6	−2.5
12 101.50	$3d^2$	$^3P_1$	−107.3	−1.8	+ 98
12 154.42	$3d^2$	$^3P_2$	−27.9	85.9	+ 408
14 261.32	$3d^2$	$^1G_4$	135.2	143.2	+ 5.9
26 081.34	$3d4p$	$^1D_2^\circ$	215.7	202.4	−6.2
27 443.71	$3d4p$	$^3F_2^\circ$	366.8	309.2	−16
27 602.45	$3d4p$	$^3F_3^\circ$	205.4	193.8	−5.7
27 917.78	$3d4p$	$^3D_1^\circ$	304.0	278.3	−8.5
28 021.29	$3d4p$	$^3D_2^\circ$	125.4	165.5	+ 32
28 161.17	$3d4p$	$^3D_3^\circ$	101.4	134.4	+ 32
29 742.16	$3d4p$	$^3P_1^\circ$	257.0	167.1	+ 35
29 823.93	$3d4p$	$^3P_2^\circ$	106.3	96.6	+ 9.1
32 349.98	$3d4p$	$^1F_3^\circ$	190.6	178.2	+ 6.5

[a]Weighted average of values presented in Table II.

[b]MCDF values are calculated using the value $\mu_I=4.748\,75$ nm from Ref. 19.

TABLE VI. Comparison of experimentally observed B values with *ab initio* MCDF values.

Level (cm^{-1})	Configuration	SLJ	B values (MHz) B (observed)[a]	B (MCDF)[b]
10 944.56	$3d^2$	$^1D_2$	7(7)	14.3
12 101.50	$3d^2$	$^3P_1$	−9(3)	−11.6
12 154.42	$3d^2$	$^3P_2$	14(8)	23.2
14 261.32	$3d^2$	$^1G_4$	−52(32)	−65.4
26 081.34	$3d4p$	$^1D_2^\circ$	18(7)	8.4
27 443.71	$3d4p$	$^3F_2^\circ$	−40(14)	−47.9
27 602.45	$3d4p$	$^3F_3^\circ$	−70(18)	−52.2
27 917.78	$3d4p$	$^3D_1^\circ$	3(6)	1.1
28 021.29	$3d4p$	$^3D_2^\circ$	7(7)	−4.7
28 161.17	$3d4p$	$^3D_3^\circ$	−23(12)	−5.5
29 742.16	$3d4p$	$^3P_1^\circ$	9(7)	9.5
29 823.93	$3d4p$	$^3P_2^\circ$	−24(18)	−17.0
32 359.98	$3d4p$	$^1F_3^\circ$	−69(34)	−67.0

[a]Weighted averages of values shown in Table II. Values in parentheses are estimated uncertainties based on the B (observed) in Table II.
[b]MCDF values are calculated using $Q = -0.22b$ from Ref. 19.

dominant contribution.

It is therefore concluded that the strong contact component of the hfs of the $3d^2$ triplet states is due to core polarization. Unfortunately, MCDF calculations of core polarization are difficult to carry out in view of the large number of configurations involved and the associated numerical stability problems. Core polarization is probably also a factor in the $3d4p$ configuration, even though the effects of CI are not as well understood due to severe numerical convergence problems. The $4p$ contact term derived from the EO analysis is large and opposite in sign to that for $3d$. A partial cancellation of the contributions may then occur, leading to the sometimes fortuitous agreement between experiment and theory.

Above, we have hypothesized that the main source of discrepancy between the observed and MCDF calculated values for the A's of the triplet states is the omission of core polarization effects in the present treatment. In support of this are the detailed calculations on the $4s4p$ configuration in Ca I, where core polarization is found to dominate the contact contribution of the p electron.[12]

Table VI shows the experimental and calculated MCDF results for the B values. Because the observed hfs splittings are dominated by the magnetic-dipole interaction, the uncertainties in the B values are large enough that for most levels the calculated and observed B's are essentially in agreement. It would be of great value to obtain more precise B values by, for example, the laser-rf double-resonance method. Comparisons between the observed and calculated B values can reveal the breakdown of LS coupling, as well as contributions from configuration-interaction and Sternheimer shielding effects. Detailed testing of the MCDF B values must await more precise experimental values.

CONCLUSION

Collinear laser–ion-beam spectroscopy has been used to measure hyperfine structure in the $3d^2$ and $3d4p$ configuration in Sc II. The experimentally observed magnetic-dipole (A) and electric-quadrupole (B) hyperfine interaction constants have been compared with those obtained from multiconfiguration Dirac Fock *ab initio* calculations. While good agreement is obtained for the A values of the singlet states in both the $3d^2$ and $3d4p$ configurations, the MCDF predictions for the triplet states are not even qualitatively correct. This apparently results from the fact that the presently used MCDF code has difficulties in accounting for core polarization effects in a fully self-consistent manner. The effective operator treatment of the data confirms this conclusion. Due to large experimental uncertainties, the observed B values are essentially in agreement with MCDF predictions. More accurate B values, which could be obtained by the laser-rf double-resonance technique, are required for a true test of the MCDF theory.

While the MCDF theory is a reasonable starting point for understanding this quasi-two-electron atom, it has problems in explaining the experimentally observed magnetic dipole hfs. With the advent of more accurate data, especially for the B values, we hope to stimulate theoretical effort, perhaps using many-body perturbation theory, on this relatively simple atom where pair correlation could be studied.

ACKNOWLEDGMENT

This work was supported by the U.S. Department of Energy, Office of Basic Energy Sciences, under Contract No. W-31-109-ENG-38.

*Present address: University of Lund, Lund, Sweden.

[1]E. W. Otten, Nucl. Phys. A **354**, 471 (1981).
[2]K. W. Dorschel, H. Hühnermann, E. Knobl, Th. Meier, and H. Wagner, Z. Phys. A **302**, 359 (1981).
[3]K. W. Dorschel, W. Heddrich, H. Hühnermann, E. W. Peau, and H. Wagner, Z. Phys. A **317**, 223 (1984); **312**, 269 (1983).
[4]U. Nielsen, K. T. Cheng, H. Ludvigsen, and J. N. Xiao, Phys. Scr. **39**, 776 (1986).
[5]S. Johansson and U. Litzén, Phys. Scr. **22**, 49 (1980).
[6]G. C. Marsden, E. A. Den Hartog, J. E. Lawler, J. T. Dakin, and V. D. Roberts (unpublished).
[7]O. Vogel, L. Ward, A. Arnesen, R. Hallin, C. Nordling, and A. Wannstrom, Phys. Scr. **31**, 166 (1985).
[8]A. Arnesen, B. Bengtsson, L. J. Curtis, R. Hallin, C. Nordling, and T. Noreland, Phys. Lett. **56A**, 355 (1976).
[9]H. P. Palenius, L. J. Curtis, and L. Lundin, J. Phys. B **9**, L473 (1976).
[10]R. Buchta, L. J. Curtis, I. Martinson, and J. Brzozowski, Phys. Scr. **4**, 55 (1971).
[11]S. Salomonson, Z. Phys. A **316**, 135 (1984).
[12]G. Olsson and S. Salomonson, Z. Phys. A **307**, 99 (1982).
[13]A. Arnesen, R. Hallin, C. Nordling, Ö. Staaf, L. Ward, B. Jelénkovic, M. Kisielinski, L. Lundin, and S. Mannervik, Astron. Astrophys. **106**, 327 (1982).
[14]L. Young, W. J. Childs, H. G. Berry, C. Kurtz, and T. Dinneen, Phys. Rev. A **36**, 2148 (1987).
[15]P. G. H. Sandars and J. Beck, Proc. R. Soc. London, Ser. A **289**, 97 (1965).
[16]The relevant matrix elements are given by W. J. Childs, Phys. Rev. A **2**, 316 (1970).
[17]K. T. Cheng and W. J. Childs, Phys. Rev. A **31**, 2775 (1985).
[18]J. P. Desclaux, Comput. Phys. Commun. **9**, 31 (1974).
[19]G. H. Fuller, J. Phys. Chem. Ref. Data **5**, 835 (1976).
[20]J. Bauche and B. R. Judd, Proc. Phys. Soc., London **83**, 145 (1964).